Journal of Atomic and Molecular Sciences

Global Science Press

ISSN 2075-1303

External electric field-dependent photoinduced electron transfer of Oligonaphthofurans-$PC_{70}BM$ in BJH solar cell

Received: July 28, 2017,
Accepted: September 20, 2017

DOI: 10.4208/jams.072817.092017a

http://www.global-sci.org/jams/

Li Yang[a], Jing Wang [b], Meixia Zhang [a], Meiyu Zhao [c] Yumei Dai [d] and Peng Song [a,*]

Abstract. To rely mainly on the impact of external electric field derived from the electronic coupling charge transfer rate in the change, the new theoretical method can not merely a better understanding of chemical structure the, external electric field and optoelectronic properties of donor(D)- acceptor(A) system , but also can be used for reasonable design of D-A system of novel organic solar cells. This article selects $PC_{70}BM$ (phenyl-fullerenes-butyric acid methyl ester) (good solubility, high electron mobility, with common polymer material to take shape a fine phase separation) as this acceptor; low five different kinds of chain length of oligonaphthofurans molecules (active material of fluorescent probe molecule) as the donor, using density functional theory on the basis of the Marcus theory to calculate the electronic coupling ,reorganization energy, gibbs free energy of reaction ,rates of the charge recombination and the rates of exciton dissociation for this study.

1. Introduction

Organic solar cell (OSCs) materials, with many advantages and potential application values, have caught great attentions recent years [1-3]. One of promising futures in this research area, is the development of novel photoactive materials in OSCs devices, which will further lower the manufacturing cost and enhance the efficiency of the device [4,5]. From the conversion efficiency close to 1% in 1986 to consecutive refreshment of the world record (～8.3% and 9.8%) in 2010 and 2011, the OSCs have gained enormous progress rapidly and its conversion efficiency has reached the level of traditional amorphous silicon solar cells. Fluorescent materials, in most cases, possess significant absorbing efficiency in the visible region. For instance, the organic photochromic naphthopyran luminescent compounds have an importantly developing prospect in the fields of optical information storage, fluorescent switch, optical brake, et al., also have been widely used in environmental monitoring and the preparation of photosensitive materials [6,7].

In the process of complex photoelectric conversion of OSCs devices, the photoinduced excited electron transfer (ET) in photoactive materials is one of most important factors in determining its efficiency. Theoretically, Marcus ET theory is the widely used model to investigate the ET reaction, not involving the chemical bond rupture and form in this process.

Marcus model expressed energy molecules of system is how to influence the change of reaction and the molecular of adjacent structure by simple mathematical formula, theory and mathematics related theory and experimental value, calculating and explaining the electron transfer reaction to photoinduced charge transfer rate by measurement.

Photoelectron between the donor (D) and acceptor (A) produce weak coupling and transfer, electron transfer reaction rates are related to the parameters such as alter of gibbs free energy and reorganization energy. In Marcus theory, the expression of the charge transfer rate is :

$$k = \sqrt{\frac{4\pi^3}{h^2 \lambda k_B T}} |V_{da}|^2 \exp\left(-\frac{(\Delta G + \lambda)}{4\lambda k_B T}\right), \quad (1)$$

where h is the Planck constant, λ is the reorganization energy, k_B is the Boltzmann constant, T is the temperature (T=300K), V_{da} is the electronic coupling matrix element between the A and the D [8], ΔG is the gibbs free energy change for the electron transfer reaction.

According to the double potential well model ,the activation free energy, reorganization energy and the heat of reaction have the relationships as follows :

$$\Delta G^* = \frac{(\Delta G + \lambda)^2}{4\lambda}, \quad (2)$$

We can know the size relationship from the above formula between gibbs free energy and reorganization energy. Therefore electron transfer will have the three conditions as follows: (1) Normal area: the more exothermic reaction, activation energy is smaller, the faster the reaction rate. For the same position to λ and ΔG is gradually increasing from positive to negative parabola. There is two cases .The one is $\Delta G > 0$, the other is $\Delta G < 0$, but the both cases are $\lambda+\Delta G > 0$. So the reaction rate constant is small, but the second one could be slightly greater than the first one. (2) Incompetent base area: the reaction rate is the fastest. When ΔG become more negative, the $\lambda+\Delta G$ become more close to zero, reaching the maximum rate constant. (3) Reverse area: unlike general reaction, heat release, The more heat release, the greater the activation energy, the slower the reaction rate. If ΔG continues to become more negative, the value of $\lambda+\Delta G$ is negative. The

[a] Department of Physics, Liaoning University, Shenyang 110036, P. R. China. songpeng@lnu.edu.cn
[b] Department of Chemistry, Liaoning University, Shenyang 110036, P. R. China.
[c] Institute of Theoretical Simulation Chemistry, Academy of Fundamental and Interdisciplinary Sciences, Harbin Institute of Technology, Harbin 150080, China
[d] Normal College, Shenyang University, Shenyang 110044, China

activation energy of electron transfer reaction falls into Marcus inversion area.

Assigning $\lambda=\lambda_{CR}$ or $\lambda=\lambda_{CT}$, and $\Delta G=\Delta G_{CR}$ or $\Delta G=\Delta G_{CT}$, for charge reorganization or exciton dissociation, respectively. In the case of weak interaction, following Fermi's Golden Rule, the rate of electron transfer is predicted to be proportional to $|V_{da}|$ [9,10,11]. Because electronic coupling V_{da}, gibbs free energy of electron transfer reaction, reorganization energy, is determined, thus the charge transfer rate can be determined under the external electric field dependent applied.

So we can further to study the correlation properties of the excited state of light induced charge transfer rate for the oligonaphthofurans-$PC_{70}BM$ molecular system and to further discussion the mechanism of light induced energy transfer and the charge transfer rate and so on. The typical fluorescent materials oligonaphthofurans was selected as the electron donor (D) and $PC_{70}BM$ as the electron acceptor (A).

2. Theoretical methods

In the process of the completion of all of the quantum chemistry calculation were performed by the Gaussian 09 software [12].The ground-state equilibrium geometries of the oligonaphthofurans-$PC_{70}BM$: $PC_{70}BM$ BHJ material (isolated $PC_{70}BM$ presented in Figure 2.1(a)) and the five oligonaphthofurans (2mer, 3mer, 4mer, 6mer, 8mer) presented in Figure 2.1(b) were optimized using density functional theory (DFT) [13] with a 6-31G(d,p) basis set and a B3LYP functional [14,15]. And then use Materials Studio 7.0 to integration for five oligonaphthofurans molecules and $PC_{70}BM$ polymer. The electronic transitions of the oligonaphthofurans : $PC_{70}BM$ and the geometry optimization of the lowest excited state of the isolated donor and the radical cation state were performed with time-dependent DFT (TD-DFT) [16], long-range-corrected functional (CAM-B3LYP) [17] and the 6-31G(d,p) basis set, separately. This five oligonaphthofurans: $PC_{70}BM$ were defined as “2OP”, ”3OP”, “4OP”, “6OP”, “8OP” and presented in Figure 2.1(c). By calculating the related value of the free energy, we explored the related properties of the charge transfer rate. In the cases of applying electric field (from -15×10^{-5} to 15×10^{-5} au) . By selecting the B3LYP function and 6-31 g (d, p) basis set to calculate the single point to the same theoretical level [18]. Using the 3D real space analysis method to explain charge transfer and energy transfer mechanism of optical functional materials in the excited state.

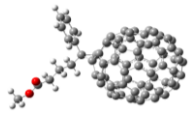

(a)

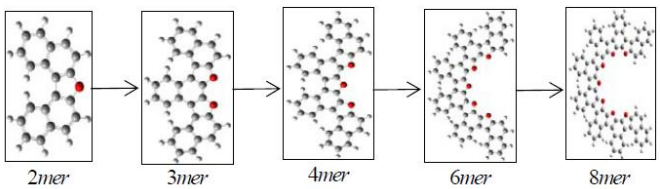

(b)

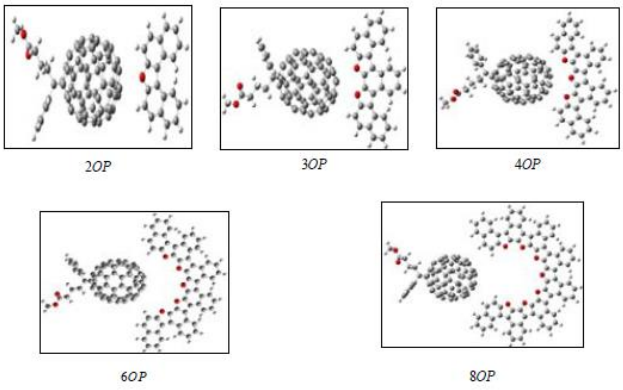

(c)

Figure 2.1: The chemical structure of (a) $PC_{70}BM$, (b) oligonaphthofurans, and (c) 2OP, 3OP, 4OP, 6OP, 8OP respectively.

3. Results and discussion

3.1 Excited state properties analysis

Due to the organic matter in each unit of the electron orbital energy level will directly affect the nature of the excited state, so the whole vertical absorption process of the HOMO and LUMO energy is very important. By using time-dependent density functional theory B3LYP function of 6-31 g (d, p) basis set, theory to calculate excited state properties of five kinds of macromolecular and analysis of each molecule LUMO energy levels, HOMO energy level and HOMO-LUMO energy gap [19] and five kinds of macromolecular system change with electric field.

Along with the change of the number of molecules of furan ring of five kinds of macromolecular HOMO energy level and LUMO energy levels, HOMO-LUMO energy level difference is changed accordingly and can calculate the 2OP, 3OP, 4OP, 6OP, 8OP of HOMO and LUMO energy level. The five kinds of macromolecular the frontier orbital energy level in zero electric field are shown in Figure 3.1.1, it can be seen on the premise that with the increase of macromolecular of furan ring number the HOMO and LUMO energy gap decreased with the electric field strength (HOMO increases changes greatly and the absolute value became smaller with the number of conjugated chain add. The LUMO change value is not big, as can be seen from the Figure 3.1.1). Because the reduce of the energy gap difference result in the addition of the wavelength, namely as HOMO-LUMO energy gap reduces, wavelength add, and so a red shift had taken place; HOMO-LUMO energy gap increases, the wavelength decreases, and a blue shift had taken place. The effect of chain length on HOMO, LUMO energy level difference (See Figure S1) at all kinds of electric field and also made a comparative analysis. This change rule and zero field change rule have the conformity change rule. HOMO-LUMO energy level difference is decreasing with the increases of the chain. The red shift of the excited state absorption spectra will accelerate the charge transfer.

The influence of electric field on the HOMO and LUMO almost can be ignored (See Figure S2). Taking 2OP and 6OP as examples in Figure 3.1.2(a) and 3.1.2(b), with the increase of electric field, HOMO and LUMO hardly change (the energy

level difference of five kinds molecular is 0.11 ~ 0.20 in the electric field -15×10^{-5}au ~15×10^{-5}au).

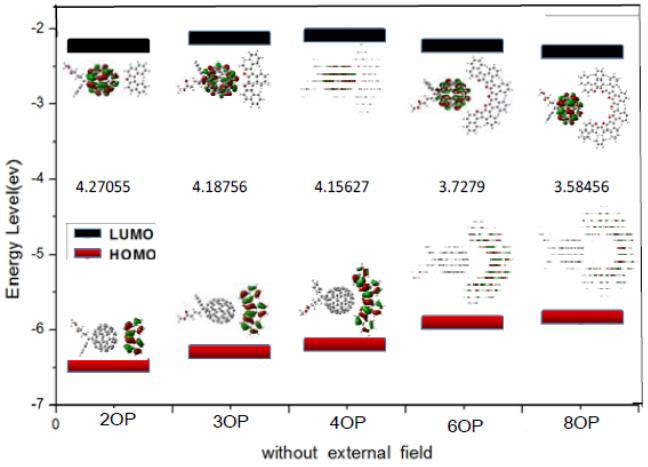

Figure 3.1.1: Molecular orbital distributions in the forefront of the system at F_{ext}=0 au.

Combined the influence of electric field and the conjugate chain length for HOMO-LUMO energy level difference, there have been a regular that conjugated chain has a larger influence on it. Because the energy difference for 2OP to 8OP is 3.4 ~ 4.4 eV, this is larger than the influence of electric field (the effect of electric field is 0.11 ~ 0.20 eV). So the effects of the conjugate chain on the HOMO-LUMO energy level difference play a leading role.

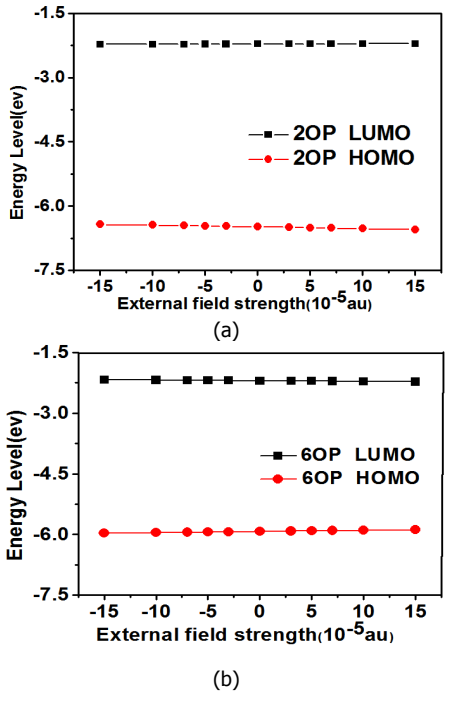

Figure 3.1.2: The HOMO and LUMO energy levels of (a) 2OP and (b) 6OP plotted versus the external electric field

Analogy optical properties of five kinds of macromolecular are presented in the Table 3-1. The excited states polymer there are two modes: one kind is intramolecular charge transfer, electrons and holes distribute on donor and acceptor, respectively; the other is a local area, this kind of excited electrons and holes transfer within the molecule. For the theoretical analysis of the nature of polymer molecules excited states, further study the excited state properties of molecular system, by using 3D solid space analysis method.

Through the analysis Figure 3.1.2 and the Table 3-1, we can clearly see that charge have taken place, namely the charge transfer. The charge transfer refers to the material absorbs light and transitions, after the transition to the excited states, and then occupied the location of the excited state molecules.The located in the excited state molecules will adjust its charge distribution, and namely the charge transfer take place ,for purpose of maintain stability. The charge transfer includes two kinds, one is intramolecular charge transfer (ICT) and the other is intermolecular charge transfer (LE).

By comparing of several states up and down from Figure 3.1.2 as we can see : for the electric field at F_{ext} =-15×10^{-5} ~ 10×10^{-5} au of 2OP ,the electron transfer is not purely the charge transfer between the molecules, because there are holes on the $PC_{70}BM$;for electric field at F_{ext} =15×10^{-5}au for S_{23} is intramolecular charge transfer, because the electron and hole are distributed on the $PC_{70}BM$. For the electric field at F_{ext} = 15×10^{-5} ~ 0 au of 3OP, it belongs to the charge transfer between the molecules .Contrasting S_{25} and S_{26} for the electric field at F_{ext} =3×10^{-5}au,this belongs to intramolecular charge transfer of $PC_{70}BM$, because the electron and hole distribute on the $PC_{70}BM$, and there was no electronic and holes distribute on the oligonaphthofurans molecule. In the same way for the electric field at F_{ext} =10×10^{-5} ~ 15×10^{-5}au ,the charge transfer is the intramolecular charge transfer, because for the S_{24} and S_{25} under the same electric field ,electron and hole distribute on $PC_{70}BM$. For F_{ext} = -15×10^{-5} ~ 15×10^{-5} au of 4OP, it belongs to the charge transfer between the molecules. By comparing the S_{21} at F_{ext} = -15×10^{-5}au and the S_{20} at F_{ext} =-15×10^{-5} au for 6OP, we can know that all hole distribution on the oligonaphthofurans molecules, all electronic distribution in $PC_{70}BM$.Therefore the electron transfer under F_{ext} =-15×10^{-5} belongs to the real charge transfer between the molecules. The remaining is not really the charge transfer between the molecules. By comparing S_{16} and S_{18} for 8OP at F_{ext} =5×10^{-5}au, all the hole distribution on the oligonaphthofurans molecules, all electronic distribution on $PC_{70}BM$. Therefore the electron transfer belongs to the real charge transfer between the molecules under the electric field of F_{ext} = 5×10^{-5} au. The remaining is not really the charge transfer between the molecules. By observing and contrast five molecular charge transfer ability, we can found: the charge transfer of 2OP was full of the whole molecule, and the charge transfer of 8OP molecular occurs only in part of the molecule, ~~which~~ with the increasing of the chain, gradually reducing the charge transfer ability.

Table 3-1: Selected electronic transition energies (TE in eV) and corresponding oscillator strengths (*f*), and Orbital transition configuration interaction factor under different external electric fields (F_{ext} in 10^{-5}au)

F_{ext}		-15	-10	-7	-5	-3	0	3	5	7	10	15
2OP	TE	3.3525	3.3523	3.3522	3.3521	3.352	3.3519	3.3518	3.3517	3.3516	3.3515	3.3513
	f	0.1226	0.1221	0.1218	0.1216	0.1214	0.1211	0.1208	0.1206	0.1204	0.1201	0.1196
	CI	0.38197	0.37992	0.37867	0.37782	0.377	0.37575	0.37448	0.37364	0.37279	0.3715	0.36935
3OP	TE	3.7098	3.7099	3.7099	3.7099	3.7099	3.7098	3.7098	3.7098	3.7097	3.7097	3.7095
	f	0.5074	0.4862	0.4726	0.4631	0.4533	0.4381	0.4223	0.4114	0.4003	0.3833	0.3542
	CI	0.58589	0.57704	0.57104	0.56676	0.56225	0.55508	0.54738	0.54196	0.53632	0.52743	0.51154
4OP	TE	3.51	3.5099	3.5099	3.5099	3.5099	3.5099	3.5098	3.5098	3.5098	3.5097	3.5097
	f	0.1947	0.1880	0.1841	0.1816	0.1791	0.1753	0.1714	0.1688	0.1662	0.1622	0.1550
	CI	0.43065	0.42897	0.4278	0.42695	0.42603	0.42451	0.42281	0.42154	0.42015	0.41743	0.41331
6OP	TE	3.1471	3.1469	3.1468	3.1467	3.1466	3.1465	3.1464	3.1463	3.1462	3.146	3.1457
	f	1.3271	1.3273	1.3273	1.3273	1.3269	1.3270	1.3269	1.3266	1.3268	1.3265	1.3264
	CI	0.6403	0.63691	0.62955	0.6142	0.56067	0.56639	0.62434	0.63294	0.63663	0.63911	0.64063
8OP	TE	3.0514	3.0517	3.0519	3.052	3.0521	3.0523	3.0524	3.0525	3.0523	3.0525	3.0526
	f	0.1369	0.1654	0.1842	0.1974	0.2110	0.2305	0.2414	0.2206	0.8770	0.4333	0.4507
	CI	0.4013	0.39231	0.38436	0.37744	0.34559	0.36935	0.36379	0.36699	0.57115	0.42491	0.43282

	F_{ext} = -15	F_{ext} = -10	F_{ext} = -7	F_{ext} = -5	F_{ext} = -3	F_{ext} = 0	F_{ext} = 3	F_{ext} = 5	F_{ext} = 7	F_{ext} = 10	F_{ext} = 15
2OP	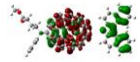	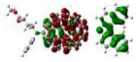	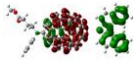	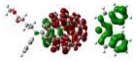	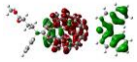	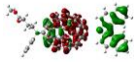	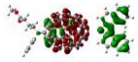	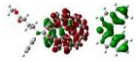	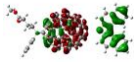	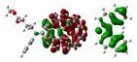	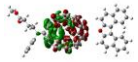
	S_{25}	S_{25}	S_{25}	S_{23}	S_{23}	S_{23}	S_{23}	S_{23}	S_{23}	S_{23}	S_{23}
3OP	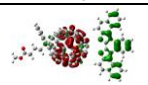	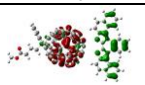	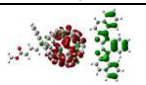	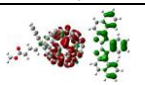	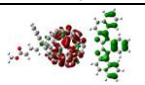	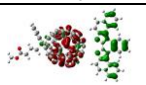	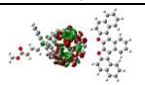	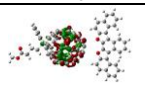	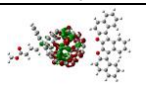	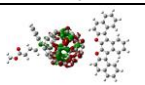	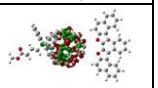
	S_{25}	S_{25}	S_{25}	S_{25}	S_{25}	S_{25}	S_{25}	S_{25}	S_{25}	S_{25}	S_{25}
4OP	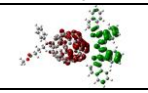	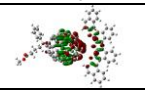	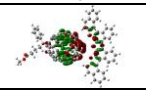	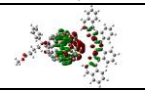	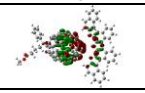	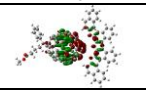	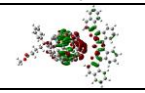	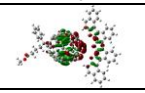	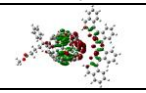	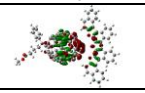	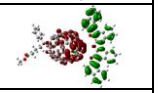
	S_{28}	S_{28}	S_{28}	S_{28}	S_{28}	S_{28}	S_{28}	S_{28}	S_{28}	S_{28}	S_{28}
6OP	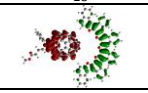	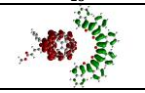	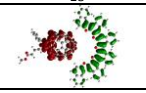	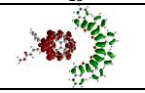	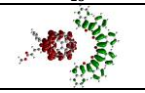	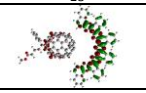	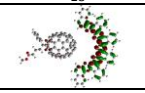				
	S_{21}	S_{21}	S_{21}	S_{21}	S_{21}	S_{21}	S_{21}	S_{21}	S_{21}	S_{21}	S_{21}
8OP											
	S_{17}	S_{17}	S_{17}	S_{17}	S_{17}	S_{17}	S_{17}	S_{17}	S_{16}	S_{16}	S_{16}

Figure 3.1.2: Selected CDDs of Oligonaphthofurans-$PC_{70}BM$ dyads at different external electric fields (F_{ext} in 10^{-5}au). Green and red color represents the hole and electron,respectively.

3.2 Charge generation and recombination rates

One route to enhance the device performance is by understanding the device physics and then optimizing the device parameters [20]. Based on the analysis for electron transfer, the electron transfer rate relies on three key parameters: reorganization energy λ, gibbs free energy ΔG, and the charge-transfer integral V_{da}. The processes of the charge transfer (CT) and the charge recombination (CR), together decide the power conversion efficiencies. Thus, λ and ΔG should be respectively handled for forward or backward reactions, with the value of $\lambda=\lambda_{CR}$ or $\lambda=\lambda_{CT}$, and $\Delta G=\Delta G_{CR}$ or $\Delta G=\Delta G_{CT}$, respectively [21]. For these two competitive processes, potential energy surfaces (PESs) of the reactants and the products are different [22].

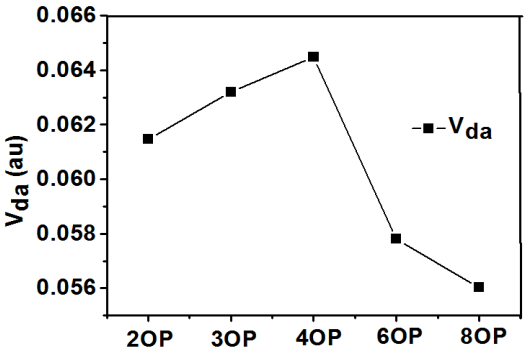

Figure 3.2.1: Electronic coupling under different conjugate chain length.

3.2.1 Electronic coupling

In organic solar cells, the charge separation occurs under the impact of the difference external electric field. One of the most important points is to investigate the external field effect on the electronic coupling [23]. By employing time-dependent density functional theory (TD-DFT) calculations of a system in uniform external electric field is capable of one analyze the electrostatic properties of molecules in their excited states [24]. Type on the second item doesn't have much of an impact on the research of light contact charge transfer rate of the qualitative results with the applied electric field control, so the second order items are not considering the TD-DFT.

Selected vertical excitation energy of S_{25} to S_{23} excited state under all electric field for combination 2OP; selected vertical excitation energy of S_{25} excited state under all electric field to combination 3OP; selected vertical excitation energy of S_{28}excited state under the all electric field for combination 4OP; selected the vertical excitation energy of S_{21} excited state under the all electric field for combination 6OP; selected the vertical excitation energy of S_{17} and S_{16} excited state under the all electric field for combination 8OP, as a transition state. Though fitting, we can get five combinations of dipole moment difference, respectively. In the above five combination formula obtained excited electronic coupling under different electric field to prepare for the rate calculation. After calculateing the 2OP, 3OP, 4OP, 6OP, 8OP at various the electric field to get the electronic coupling strength. By comparing we found that the same kind of macromolecule with the increase of electric field electron, the coupling strength there is not much change (It has changed in the fourth after the decimal point). This suggests that the electric field effect on the electronic coupling almost can be ignored. But the influence of conjugated chain length to the electronic coupling strength though small but has certain regularity. The electronic coupling figure at $\boldsymbol{F}_{ext}$=0 is presented in Figure 3.2.1. The 2OP, 3OP and 4OP presents ascendant trend, 6OP, and 8OP separately presented down trend. Their trend has broadly the uniform trend.

3.2.2 Gibbs free energy

The entirety ΔG controls the activation energy barrier of the electron transfer reaction. For efficiently quenching an electronic transition excited state and competing with other non-radiation pathways, the exothermic situation is needed [26]. So far, the theoretical simulation of two major modalities ΔG_{CT} and ΔG_{CR} in different ways were used [25-32].

In the process of exciton dissociation and restructuring, the ΔG is equal to ΔG_{CT} and ΔG_{CR} separately. ΔG_{CR} has been uncovered that it directly correlation to the ionization potential E_{IP}(D) and the electron affinity E_{EA}(A), for a bimolecular species [33]. Normally, the energy of the donor's HOMO and acceptor's LUMO are used for quantitatively reckoning them [26]. So, the ΔG_{CR} can be evaluated under the thermodynamic criteria as: [30,34-36]

$$\Delta G_{CR} = E_{IP}(D) - E_{EA}(D), \quad (3)$$

Through calculation, the value is negative at all the electric fields. This means that electronic composite process is spontaneous thermodynamics system. The absolute value of ΔG_{CR} has a tendency to decrease and with the increase of the electric field, but it is not obvious. With the adding of chain length, ΔG_{CR} adds little by little. The calculation formula of ΔG_{CT} is shown below:

$$\Delta G_{CT} = -\Delta G_{CR} - \Delta E_{0-0} - E_b, \quad (4)$$

Where $\Delta E_{0\text{-}0}$ is the donor's excited state energy, and the exciton binding energy E_b comes from the difference in the energies of the optical and electronic band-gaps [37]. E_b is represented as:

$$E_b = E_{S1} - (E_L - E_H), \quad (5)$$

So with the adding of conjugated chain length, the ΔG_{CT} negative trend is bigger and bigger; with the increase of conjugated chain length, the ΔG_{CR} negative trend is gradually bigger. The change slope of 2OP and 3OP is the largest, for all the ΔG_{CT} and ΔG_{CR}, which has the same change trend at $\boldsymbol{F}_{ext}$ = -15 ~-3×10^{-5}au that with the increase of conjugated chain length ΔG_{CT} negative trend is more and more big; but the trend has changed that the 8OP becoming positive trend is bigger and bigger at $\boldsymbol{F}_{ext}$=-3×10^{-5} ~15×10^{-5}au.The impact of

conjugated chain length to ΔG_{CT} and ΔG_{CR} at the electric field was presented in Figure S2.

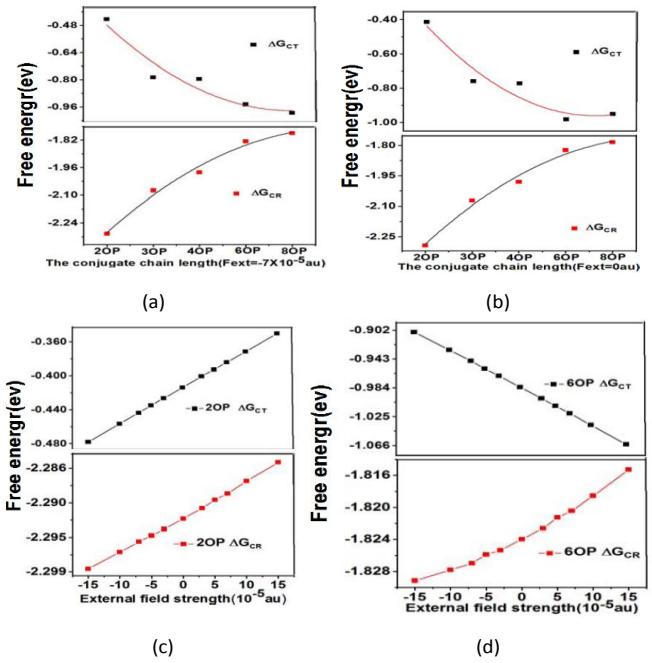

Figure 3.2.2: TheΔG_{CT} and ΔG_{CR} of different conjugated chain length at (a) F_{ext}=-7×10^{-5}au and (b) F_{ext}= 0. TheΔG_{CT} and ΔG_{CR} plotted versus the external electric field for (c) 2OP and for (d) 6OP.

As an illustration in Fig. 3.2.2(a) and (b), ΔG_{CT} and ΔG_{CR} has the same change trend, so with the increase of electric field, their becoming positive trend is bigger and bigger under the electric field .But the value of ΔG_{CR} in 6OP become negative trend is more significant with the increase of the electric field, when taken 2OP and 6OP as examples, as shown in Figure 3.2.2 (c) and (d). By comparing we found that, with the increase of conjugated chain length ΔG_{CT} basically declines, ΔG_{CR} basically rises. With the increase of electric field, ΔG_{CT} and ΔG_{CR} had almost into a rising trend for the impact of the conjugated chain length and the external electric field on ΔG_{CT} and ΔG_{CR}. By comparing the value of the conjugate chain length and electric field effect for ΔG_{CT} and ΔG_{CR}, there was a rule that the influence of conjugated chain length is bigger than electric field effect.

3.2.3 Reorganization Energy

Reorganization Energy λ is one of the important parameters to control electron or energy transfer .Reorganization Energy can as well be known as the relaxation It is the change value of energy that relaxation state $_{to}$ stable state in the whole system with the change of electron transfer. The reorganization energy comes out the deeper understanding of the driving force of the electronic transition reaction [38,39], and is primarily dedicated to the intrinsic barriers of both configuration and polarization changes, as confirmed by $\lambda = \lambda_i + \lambda_s$ [26]. The inner part of the reorganization energy λ_i is generated by changing the equilibrium geometry of donor and acceptor sites for compensating the electric charge gotten or lost upon electron transfer [40,41,42]. The outer part of the reorganization energy λ_s comes from changing the electronic and nuclear polarizations induced by the whole equilibrium geometry relaxation of solute molecules and the surrounding medium in the ET process. Normally refers to the solvent reorganization energy. The whole λ_i is gotten by meaning λ_{i1} and λ_{i2} [43, 41]. For the charge separation process, λ_i is expressed as following:

$$\lambda_{i1} = [E^{D^+}(Q_P) + E^{A^-}(Q_P)] - [E^{D^+}(Q_R) + E^{A^-}(Q_R)] , \quad (6)$$

$$\lambda_{i2} = [E^{D^+}(Q_R) + E^{A^-}(Q_R)] - [E^{D^+}(Q_P) + E^{A^-}(Q_P)], \quad (7)$$

$$\lambda_i = (\lambda_{i1} + \lambda_{i2})/2 , \quad (8)$$

Separately, Q_P and Q_R are the equilibrium coordinates of the reactants and the products. The λ_s mainly comes from overall structural (heterojunction and solvent molecules) changes causing the surrounding medium electronic polarization changes. It is hard to estimate through reliable quantitative theory. So we need to use classical medium for continuous classical model. Due to the difference of experiment conditions factors will cause the uncertainty for dielectric constant of continuum model. So the λ_s is uncertain. But the λ_s and the λ_i have the same order of magnitude. So we ought to pay attention to that the λ_s is the most uncertain factors in the calculation. We can see that with the increase of conjugated chain length, λ_{CT} and λ_{CR} have a downward trend from the Figure S5. It can be seen that λ_{CT} is greater than λ_{CR} for downward trend from the numerical, with -7×10^{-5}au and 0 au presented in the Figure 3.2.3(a) and (b). Compared respectively change trend was nearly unchanged under different electric field. We can see the effects of electric field on conjugate chain length almost can be ignored, from the in Figure S6, taking 2OP and 6OP as an example presented in the Figure 3.2.3(c) and (d). Contrasted the value and change trend for the Figure S5 and Figure S6 can be concluded that conjugated chain length of the influence of λ_{CT} and λ_{CR} is bigger than that of electric field influence.

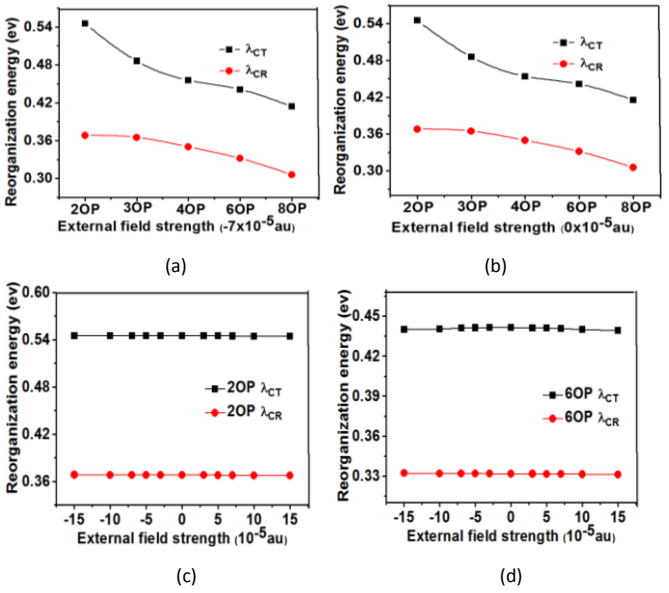

Figure 3.2.3: The λ_{CT} and λ_{CR} of different conjugated chain length at (a) F_{ext}=-7×10^{-5}au and (b) F_{ext}=0 au. The λ_{CT} and λ_{CR} plotted versus the external electric field for (c) 2OP and (d) for 6OP.

3.2.4 Rates of exciton dissociation and charge recombination

The transport of charge and exciton are all significant elementary processes in different areas of research [44, 45]. According to Marcus model, we evaluate the rate of exciton separation and the rate of charge recombination of external electric field, through equation calculation parameters. The rate of exciton separation and the rate of charge recombination of five kinds of macromolecular were calculated and then those were gotten. But electrical charge recombination rate significantly less than dissociation rate. Due to $\Delta G+\lambda$ is mainly the negative (The absolute value is very big) in Marcus inversion area. To these five macromolecular systems do not apply very well, so the paper mainly discusses the exciton dissociation rate.

Comparing the conjugate chain length changes and as the change of electric field, respectively, in these five systems. We can get from the diagram that with the increase of conjugated chain length, the exciton separation rate is declining seeing Figure 3.2.4 (a) and (b) when $\boldsymbol{F}_{ext}$=-7×10^{-5} and 0 au. With the increasing of electric field, the exciton separation rate behave differently, as can be seen in the Figure 3.2.4 (c) and (d). Based on the previous analysis, the trend should be related to ΔG^*. When strengthening external electric field, k_{CT} will rise; when ΔG^* falling with the augment of external electric field and k_{CT} will drops. Comparing k_{CT} of 2OP, 3OP and 4OP, we can see the value of k_{CT} is large. There are a few guesses: (1) 2OP may be in incompetent base area, the value of $\Delta G+\lambda$ that have 0.06695 and 0.08855 for electric field -15×10^{-5} au and~10×10^{-5} au is almost close to zero. After it ~~is~~ gradually increases with the augment of externa, the electric field may be the reason to cause the exciton separation rate decreases. The $\Delta G+\lambda$ value of 3OP, 4OP is negative (absolute value is very small), and the absolute value is smaller than 6OP, 8OP.So exciton separation rate of 3OP, 4OP will be big. (2) Oligonaphthofurans and $PC_{70}BM$ are close together, so vibrational quantum effect is increasing. (3) The influencing factors of charge transport properties include molecular structure, the molecular packing way and environment etc, not all the molecular packing are orderly arranged. For a lot of organic small molecule materials, molecular accumulation may namely the relative position between the molecular determine their transport properties. Sometimes, a little bit variation in the relative position between the molecules may induce great changes of carrier mobility.

4. Conclusions

This article is mainly based on the theory of Marcus, using density functional method, selecting $PC_{70}BM$ as acceptor and five different chain long oligonaphthofurans molecules for the donor. The photoinduced charge transfer and energy transfer mechanism were studied. The gibbs free energy of the charge transfer, recombination and the charge transfer rate was calculated. Through calculation and analysis, we found that the conjugate chain length have certain influence to the HOMO and LUMO energy levels; and with the increase of conjugated chain length, the HOMO and LUMO energy level difference decrease gradually. Electronic coupling intensity showed a trend of decrease after the first increase. For free energy show the trend that the ΔG_{CT} decreases with the increase of conjugated chain length; the ΔG_{CR} increase with the increase of conjugated chain length. For the reorganization energy λ_{CT} and λ_{CR} reduce with the incensement of conjugated chain length. These for exciton separation rate decreases with the increase of conjugated chain length caused a certain influence. The influence of the HOMO and LUMO and electronic coupling intensity, the recombination energy, gibbs free energy under electric field is not particularly big. Although the influence is small but the rate is more sensitive. 8OP is less two orders of magnitude than the other, especially. Conjugate chain length for the influence of the charge transfer mechanism need to further research.

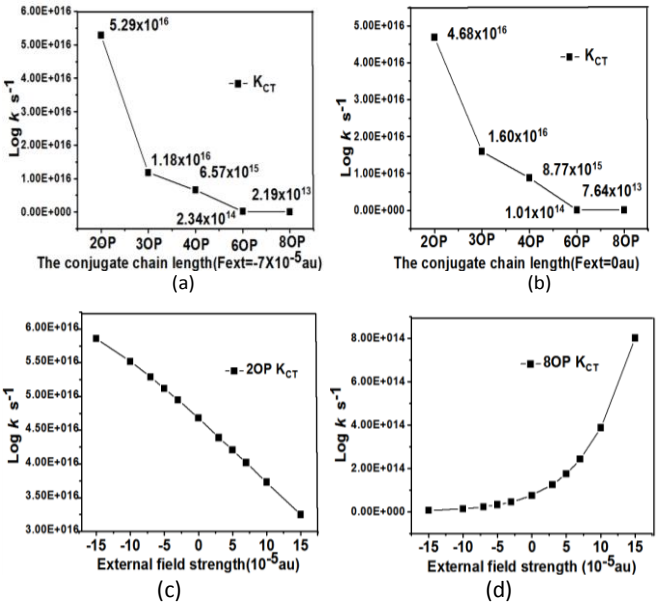

Figure 3.2.4: The k_{CT} of different conjugated chain length at (a) $\boldsymbol{F}_{ext}$=-7×10^{-5} au and (b) $\boldsymbol{F}_{ext}$=0 au. The exciton separation rate k_{CT} (c) of 2OP and (d) of 8OP, at different external electric fields.

Acknowledgements

This work was financially supported by the National Natural Science Foundation of China (Grant No. 11274149, 11304135 and 11544015), the Shenyang Natural Science Foundation of China (F15-199-1-04). Liaoning Provincial Department of Education Project (Grant No. L2015200) and the Natural Science Foundation of Liaoning Province (Grant No. 201602345 and 201601095).

References

[1] C. Brabec, U. Scherf and V. Dyakonov, Org. Photovoltaics, Wiley-VCH, Weinheim (2008).
[2] R. H. Friend, R. W. Gymer, A. B. Holmes, J. H. Burroughes, R. N. Marks, C. Taliani, D. D. C. Bradley, D. A. D. Santos, J. L.

Bredas, M. Logdlund and W. R. Salaneck, Nat., 397 (1999) 121.
[3] I. G. Scheblykin, A. Yartsev, T. Pullerits, V. Gulbinas and V. Sundström, J. Phys. Chem. B , 111 (2007) 6303.
[4] N. Blouin, A. Michaud, D. Gendron, S. Wakim, E. Blair, R. Neagu-Plesu, M. Belletête, G. Durocher, Y. Tao and M. Leclerc, J. Am. Chem. Soc., 130 (2008) 732.
[5] S. Gunes, H. Neugebauer and N. S. Sariciftci, Chem. Rev., 107 (2007) 1324.
[6] J. F. Zhang, Y. Zhou, J. Yoon and J. S. Kim, Chem. Soc. Rev., 40 (2011) 3416.
[7] J. Luo, J. Jiang and X. Y. Liu, J. Func. Polymers, 23 (2010) 1.
[8] P. Song, Y.Z. Li, F.C. Ma, and M. T. Sun, J. Mater. Chem. C., 3 (2015) 4810.
[9] G. Horowitz, Adv. Mater., 10 (1998) 365.
[10] R. A. Marcus, N. Sutin, Biochim. Biophys. Acta , 811 (1985) 265–322.
[11] M. D. Newton, N. Sutin, Annu. Rev. Phys. Chem.,35 (1984) 437–480.
[12] M. J. Frisch, et al., Gaussian 09, Revision A.1, Gaussian, Inc.,Wallingford, CT, 2009.
[13] P. Hohenberg and W. Kohn, Phys. Rev., 136 (1964) B864.
[14] A. D. Becke, Phys. Rev. A: At., Mol., Opt. Phys., 38 (1988) 3098.
[15] A. D. Becke, J. Chem. Phys., 98 (1993) 5648.
[16] E. K. U. Gross and W. Kohn, Phys. Rev. Lett., 55 (1985) 2850.
[17] T. Yanai, D. P. Tew and N. C. Handy, Chem. Phys. Lett., 393 (2004) 51.
[18] G. C. Han, K. Zhao, P. W. Liu, and L. L. Zhang, Chin. Phys. B., 21 (2012) 507.
[19] P. J. Tancell, M. R. Michael, D. P. Robin, and Jim. Braven. , Environ. Sci. Technol., 29 (1995) 2871.
[20] C. J. Brabec, et al., Adv. Funct. Mater., 11 (2001) 374 – 380
[21] P. Song, Y.Z. Li, F.C. Ma, and T. Pullerits and M. T. Sun, Chem. Rec., 16 (2016) 734.
[22] H. N. Chen, M. A. Ratner and G. C. Schatz, J. Phys. Chem. C, 115 (2011) 18810.
[23] P. Song, Y.Z. Li, F.C. Ma, and T. Pullerits and M. T. Sun., J. Phys. Chem. C, 117 (2013) 15879.
[24] F. C. Grozema, R. Telesca, F. C. Jonkman, H. T., L. D. A. Siebbeles and J. G. Snijders, J.Chem. Phys., 115 (2001) 10014.
[25] H. N. Chen, M. A. Ratner and G. C. Schatz, J. Phys. Chem. C, 115 (2011) 18810.
[26] J. K. George and J. T. Nicholas, Chem. Rev.,86 (1986) 401.
[27] M. Hilczer, S. Traytak and M. Tachiya, J. Chem. Phys., 115 (2001) 11249.
[28] X. Zhang, L. N. Chi, S. M. Ji, Y. B. Wu, P. Song, K. L. Han,H. M. Guo, T. D. James and J. Z. Zhao, J. Am. Chem. Soc.,131 (2009) 17452.
[29] T. Liu and A. Troisi, J. Phys. Chem. C, 115 (2011) 2406.
Y. Z. Li, T. Pullerits, M. Y. Zhao and M. T. Sun, J. Phys. Chem. C, 115 (2011) 21865.
[30] D. Veldman, S. C. J. Meskers and R. A. J. Janssen, Adv. Funct. Mater., 19 (2009) 1939.
[31] M. Tachiya, J. Phys. Chem., 97 (1993) 5911.
[32] K. Chibisov, Russ. Chem. Rev.,50 (1981) 1169.
[33] G. L. Gaines III, M. P. O'Neil, W. A. Svec, M. P. Niemczyk and M. R. Wasielewski, J. Am. Chem. Soc., 113 (1991) 719.
[34] A. Weller, Z. Phys. Chem., 133 (1982), 93.
[35] S. B. Li, Y. A. Duan, Y. Geng, H. B. Li, J. Z. Zhang, H. L. Xu, M. Zhang and Z. M. Su, Phys. Chem. Chem. Phys., 16 (2014) 25799.
[36] G. D. Scholes and G. Rumbles, Nat. Mater., 5 (2006) 683.
[37] R. A. Marcus, Annu. Rev. Phys. Chem., 15 (1964) 155.
[38] R. A. Marcus, J. Chem. Phys.,26 (1957) 867.
[39] P. Song, Y. Z. Li, F. C. Ma, T. Pullerits and M. T. Sun, J. Phys. Chem. C, 117 (2013) 15879.
[40] A. van Vooren, V. Lemaur, A. Ye, D. Beljonne and J. Cornil, Chem. Phys. Chem, 8 (2007) 1240.
[41] X. R. Liu, W. Shen, R. X. He, Y. F. Luo and M. Li, J. Phys. Chem. C, 118 (2014) 17266.
[42] V. Lemaur, M. Steel, D. Beljonne, J. L. Brédas and J. Cornil, J. Am. Chem. Soc., 127 (2005) 6077.
[43] M. L. M. Grage, Y. Zaushitsyn, A. Yartsev, M. Chachisvilis, V. Sundström and T. Pullerits, Phys. Rev. B, 67 (2003) 205207.
[44] M. M. L. Grage, T. Pullerits, A. Ruseckas, M. Theander, O. Inganäs and V. Sundström, Chem. Phys. Lett., 339 (2001) 96.

Journal of Atomic and Molecular Sciences

ISSN 2075-1303

Global Science Press

Supporting Information of

External electric field-dependent photoinduced electron transfer of Oligonaphthofurans-$PC_{70}BM$ in BJH solar cell

Li Yang[a], Jing Wang [b], Meixia Zhang [a], Meiyu Zhao [c] Yumei Dai [d] and Peng Song [a,*]

Received: July 28, 2017,
Accepted: September 20, 2017
DOI: 10.4208/jams.072817.092017a

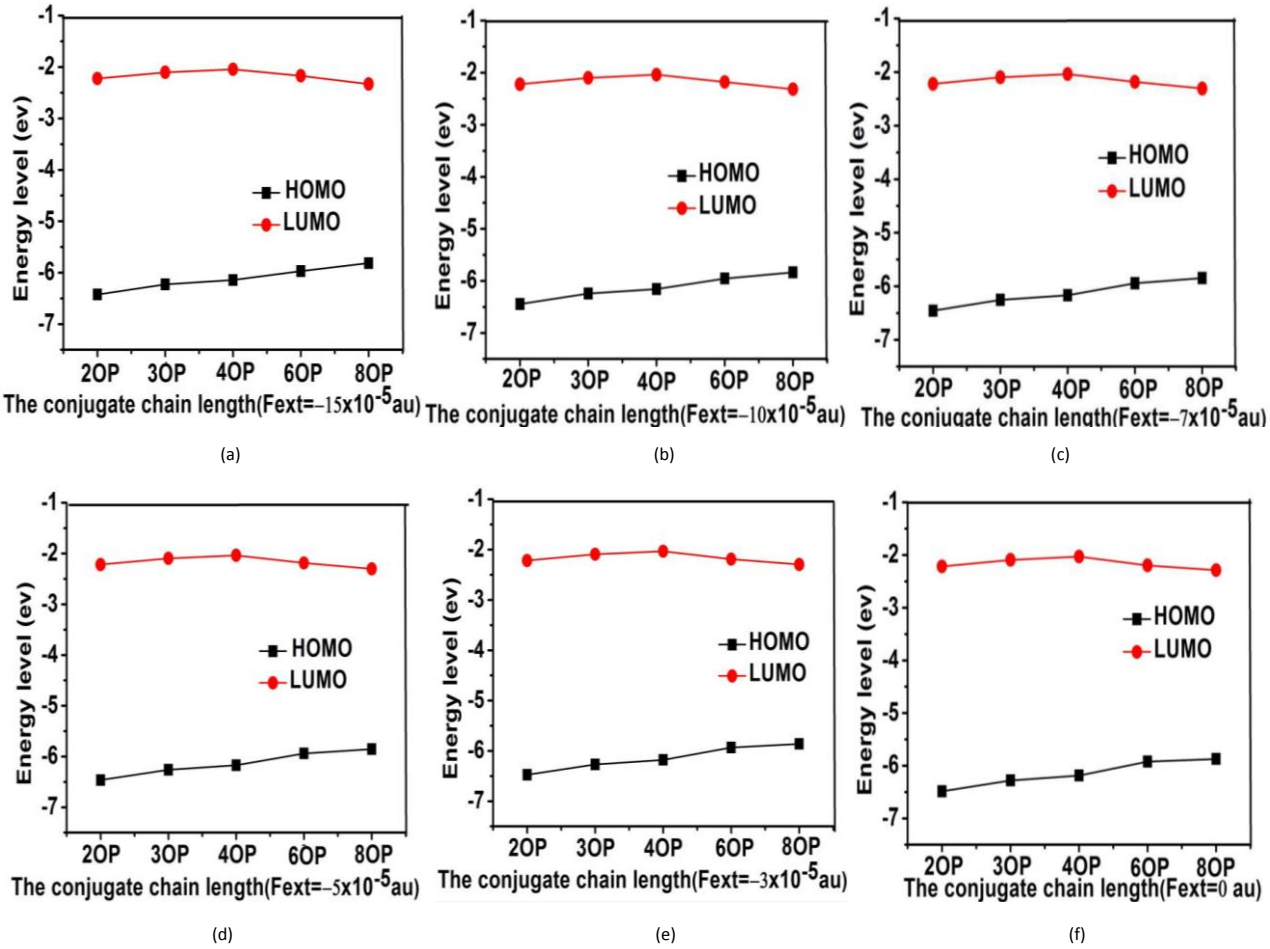

(a) (b) (c)

(d) (e) (f)

[a] Department of Physics, Liaoning University, Shenyang 110036, P. R. China. songpeng@lnu.edu.cn
[b] Department of Chemistry, Liaoning University, Shenyang 110036, P. R. China.
[c] Institute of Theoretical Simulation Chemistry, Academy of Fundamental and Interdisciplinary Sciences, Harbin Institute of Technology, Harbin 150080, China
[d] Normal College, Shenyang University, Shenyang 110044, China

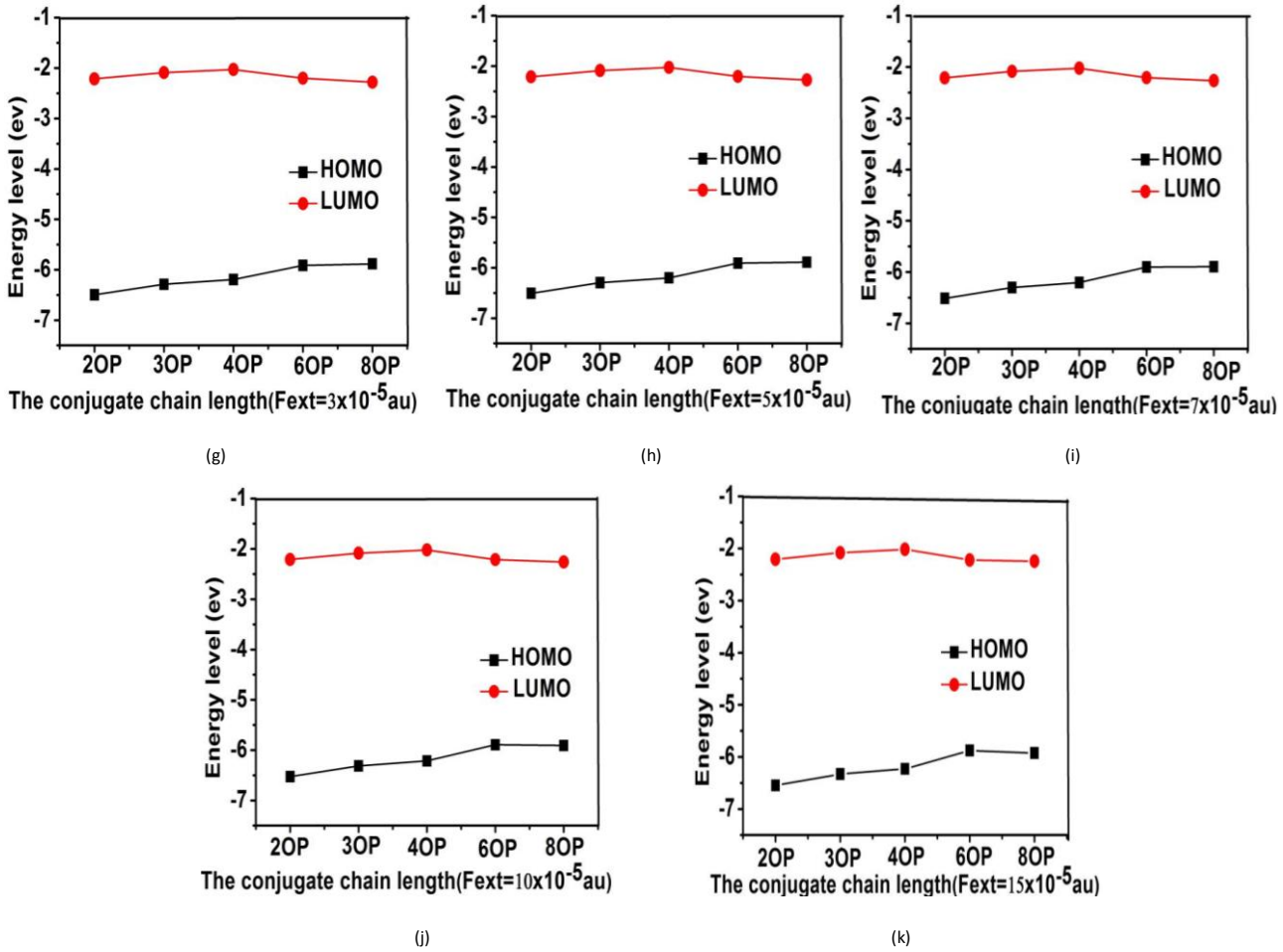

Figure S1: The forefront Molecular orbital distributions in the system at different external electric fields.

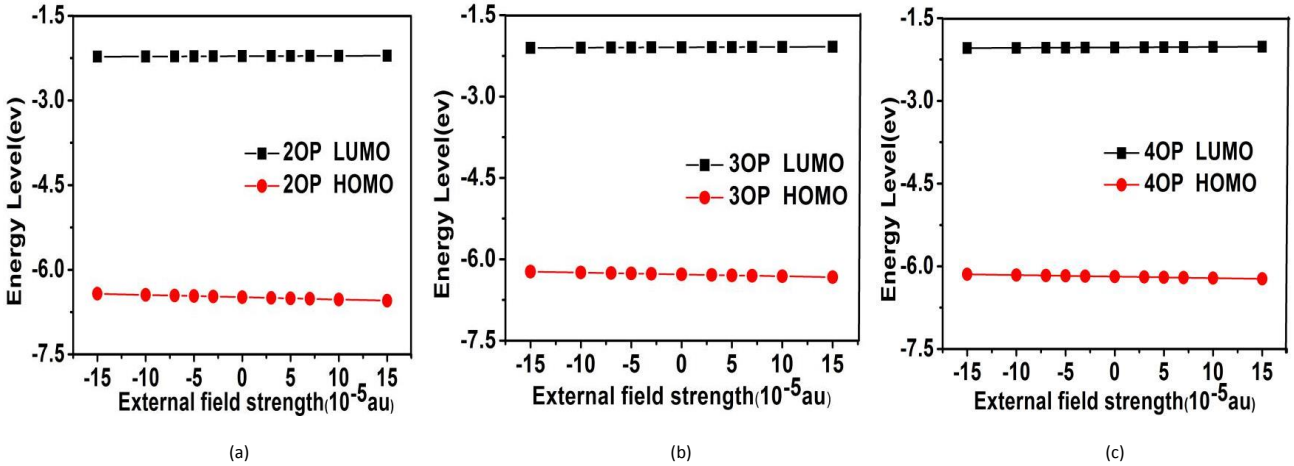

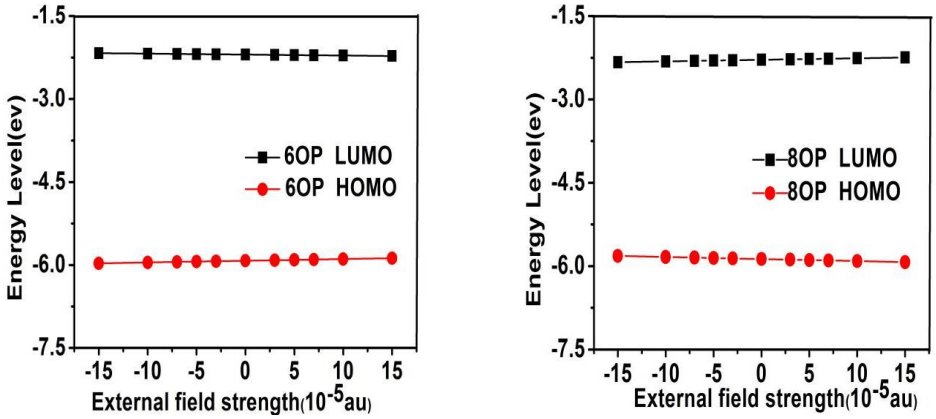

(d) (e)

Figure S2: The forefront Molecular orbital distributions in the system at different Conjugated chain length.

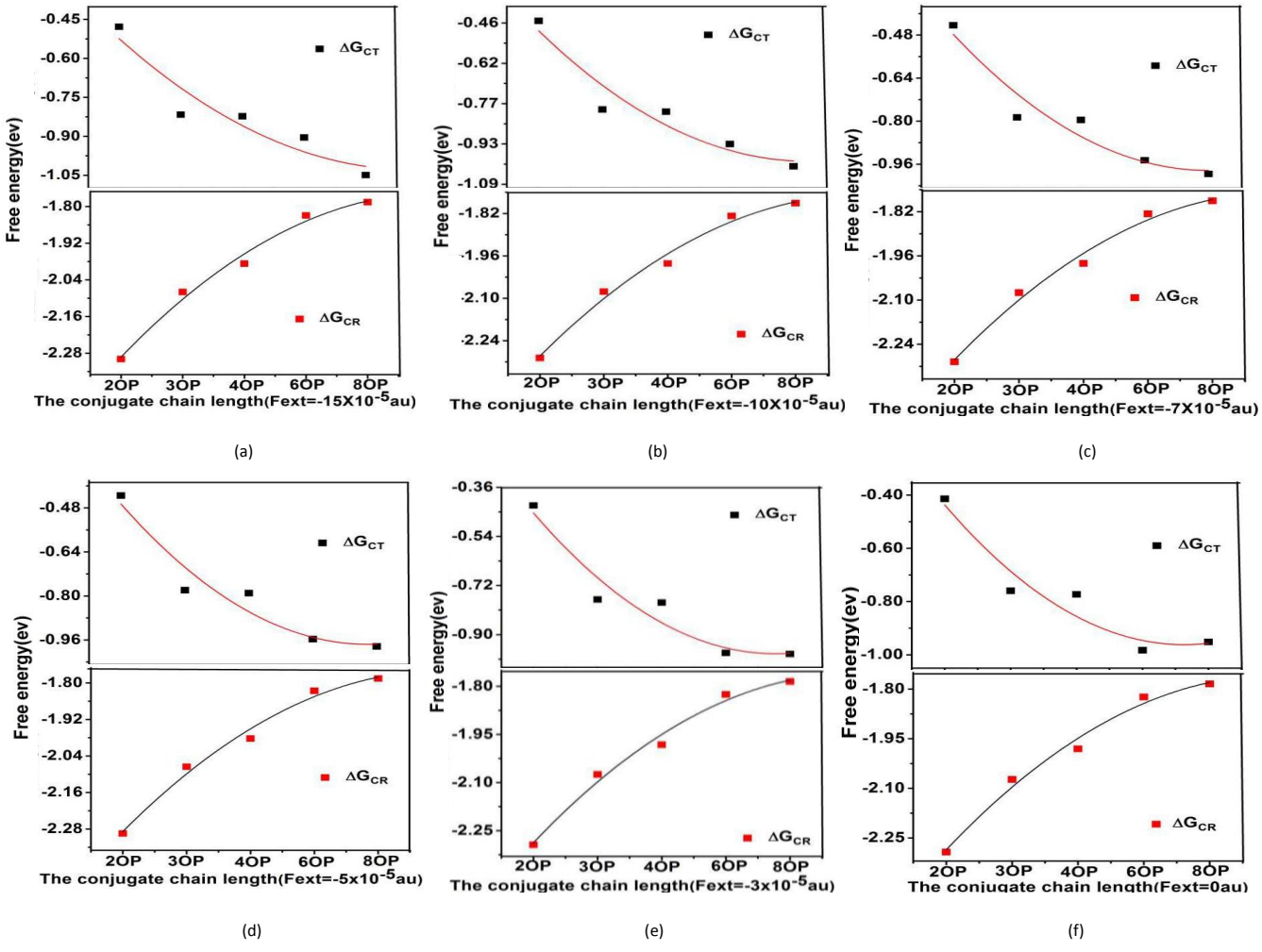

(a) (b) (c)

(d) (e) (f)

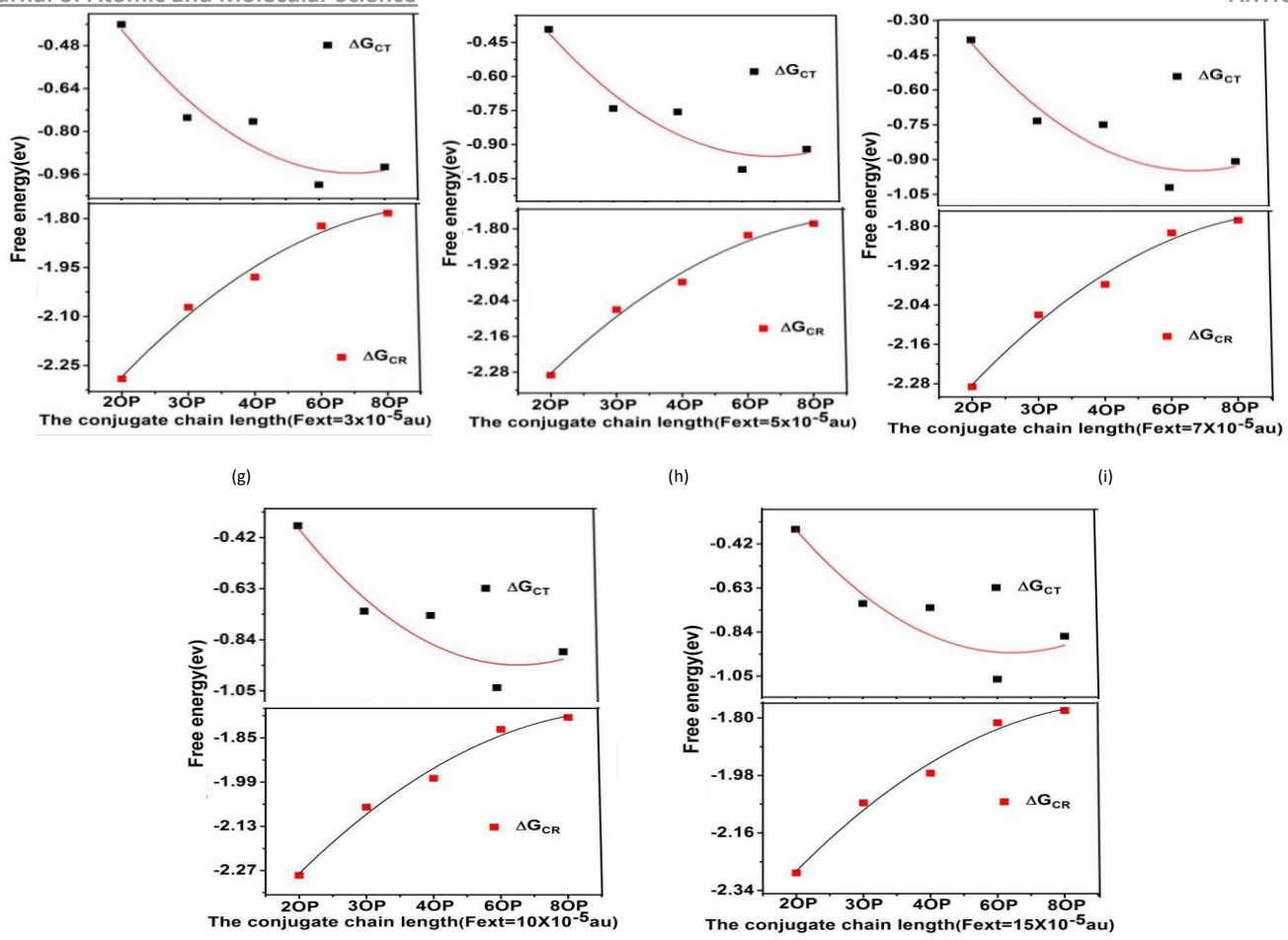

Figure S3: The ΔG_{CT} and ΔG_{CR} in the system at different external electric fields.

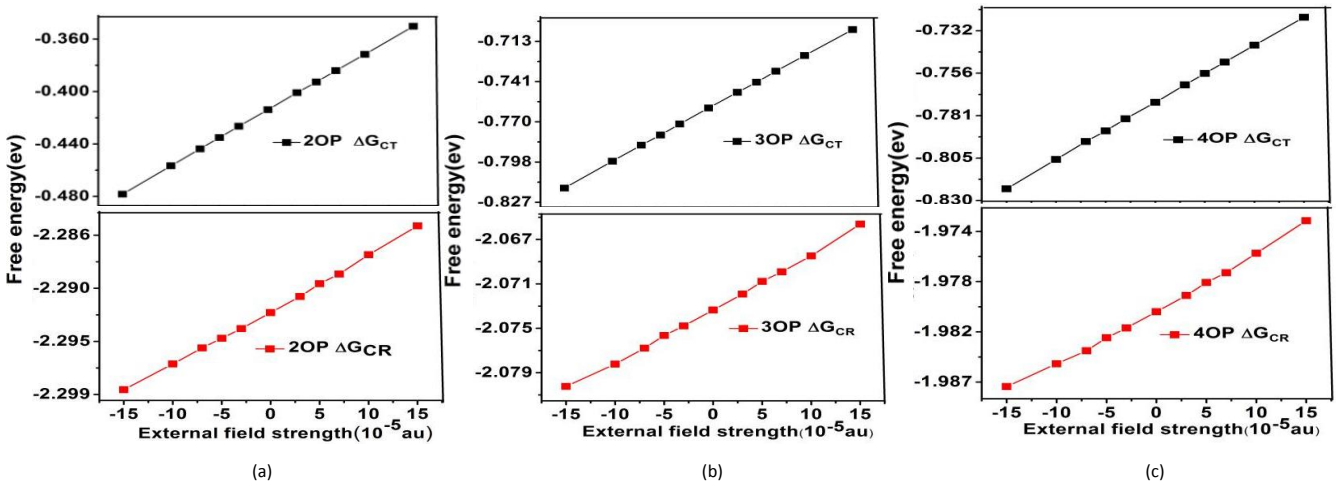

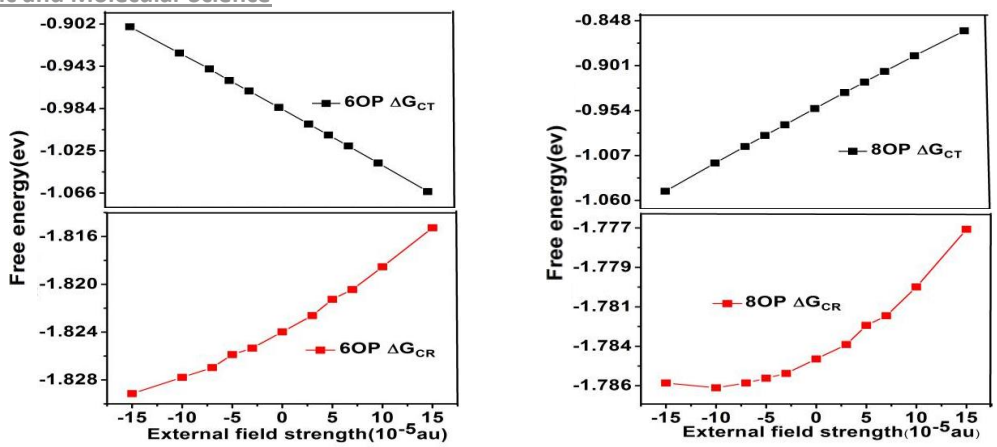

(d) (e)

Figure S4: The ΔG_{CT} and ΔG_{CR} in the system at different Conjugated chain length.

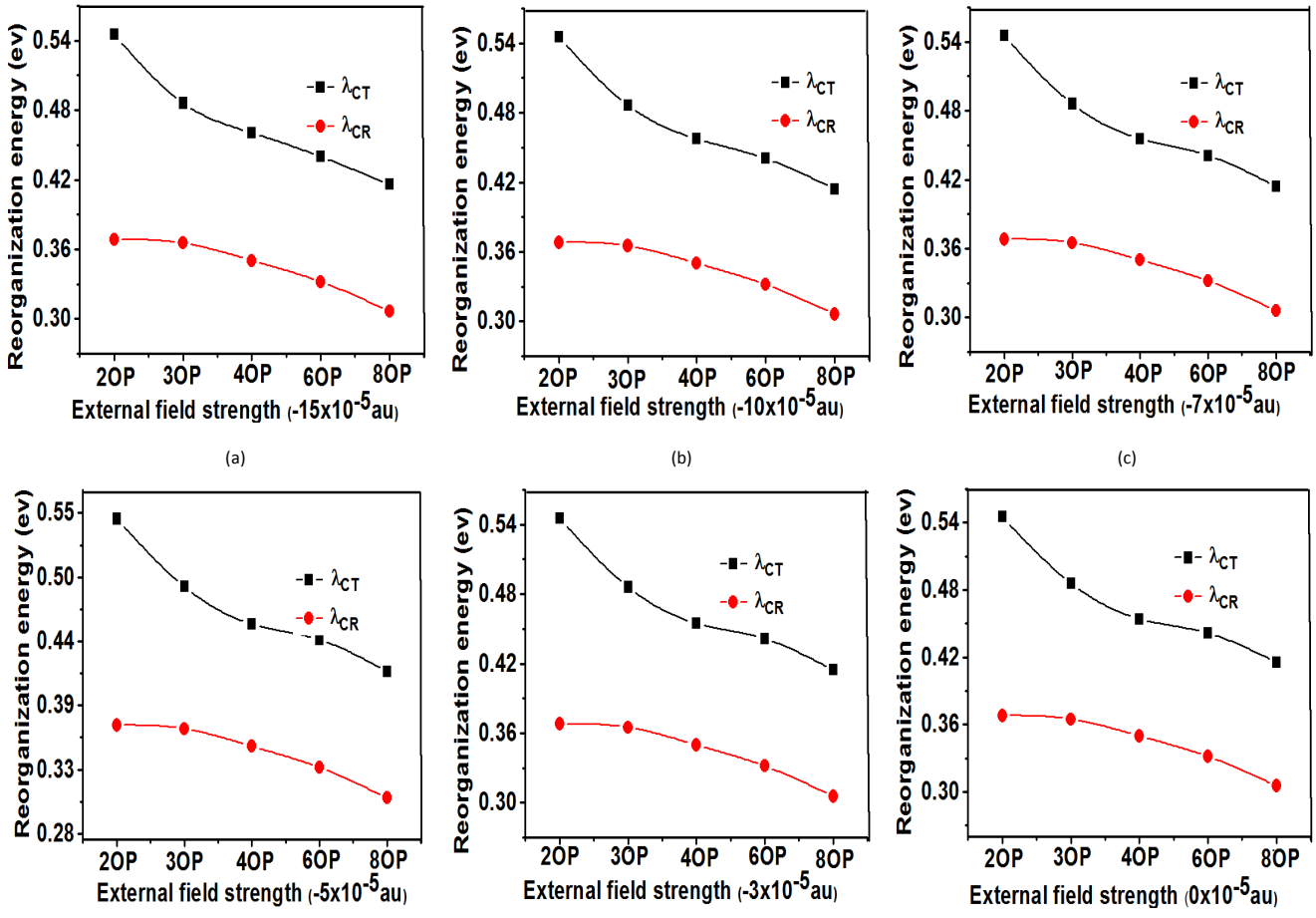

(a) (b) (c)

(d) (e) (f)

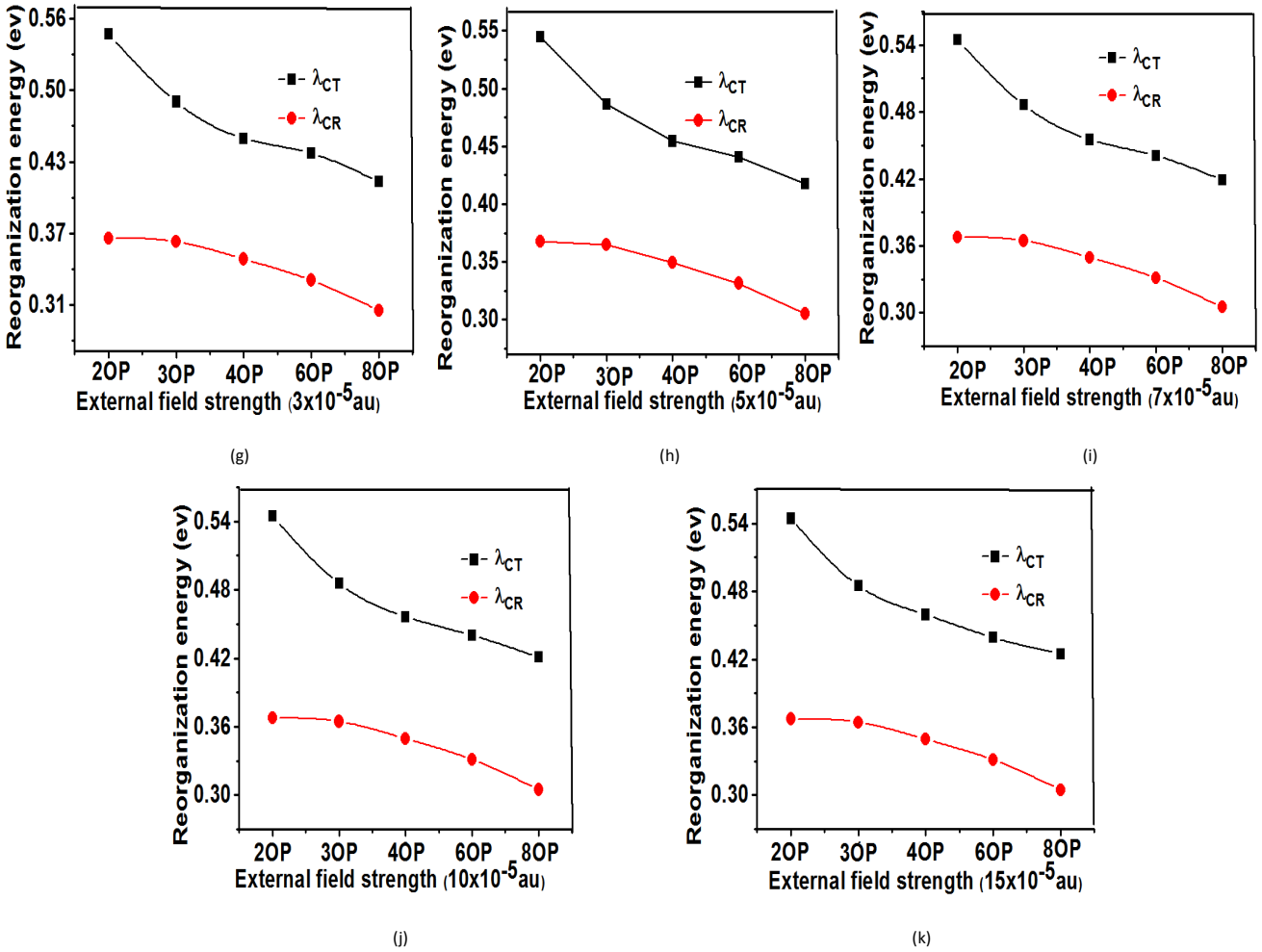

Figure S5: The λ_{CT} and λ_{CR} in the system at different external electric fields.

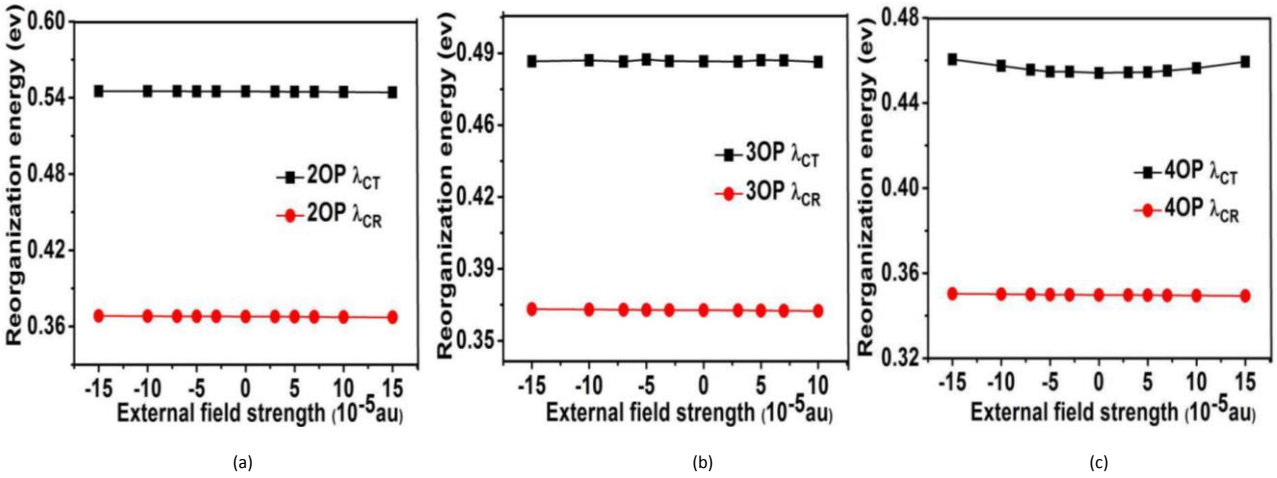

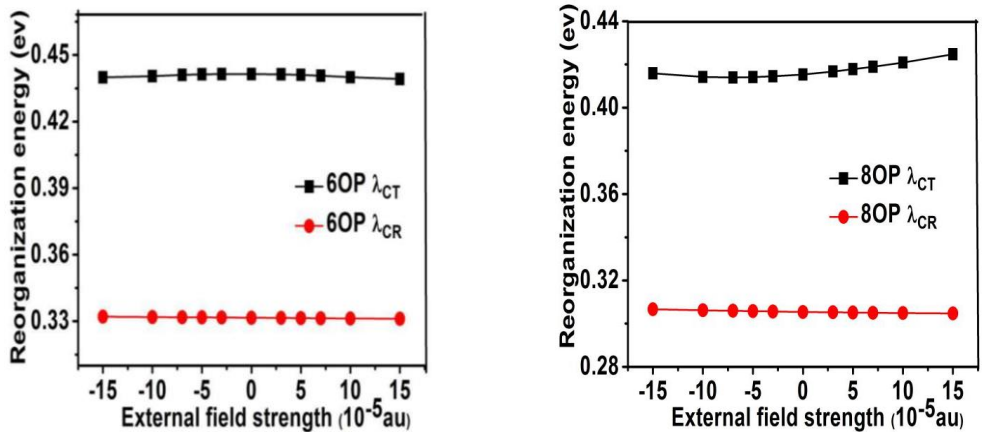

(d) (e)

Figure S6: The λ_{CT} and λ_{CR} in the system at different conjugated chain length.

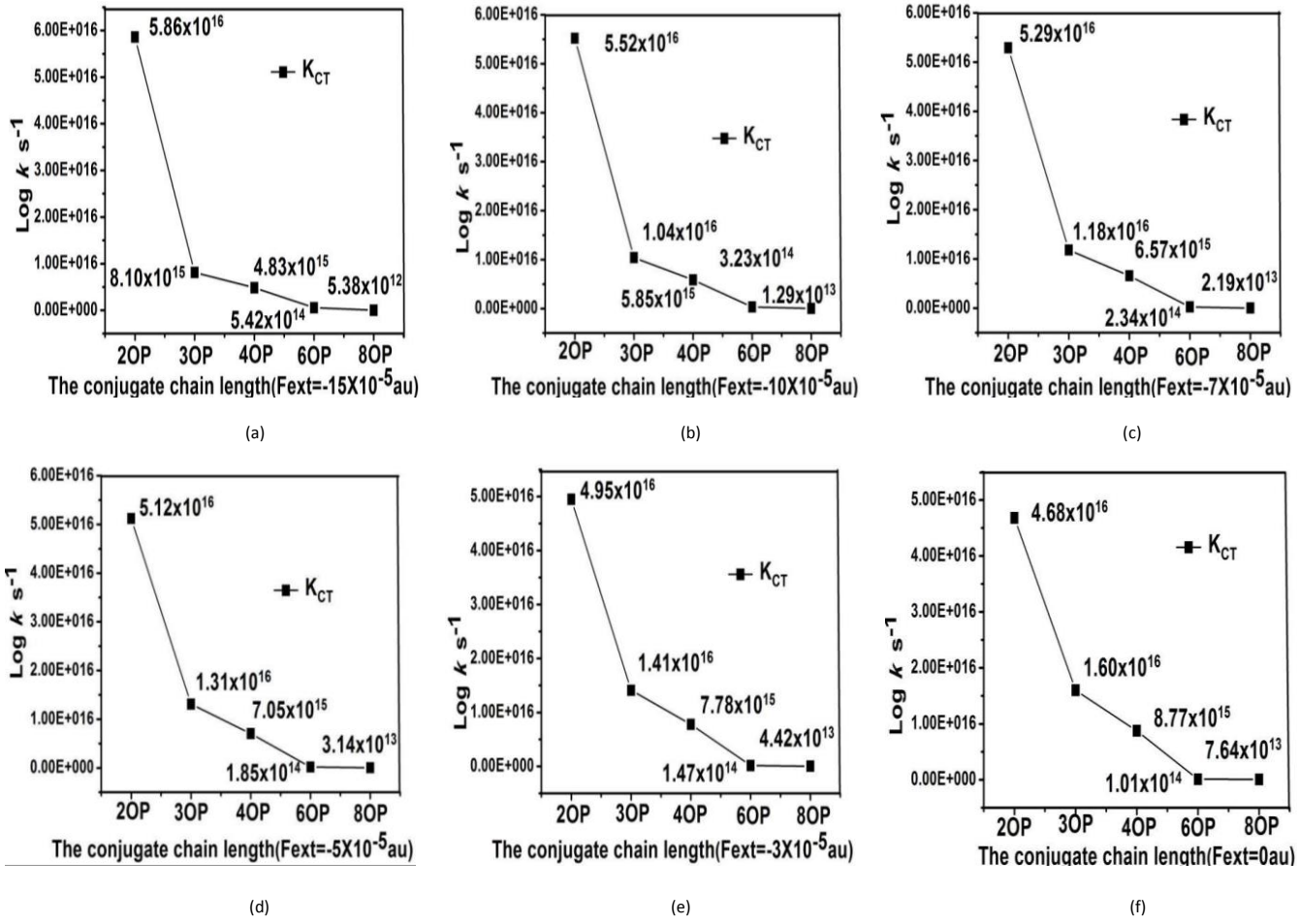

(a) (b) (c)

(d) (e) (f)

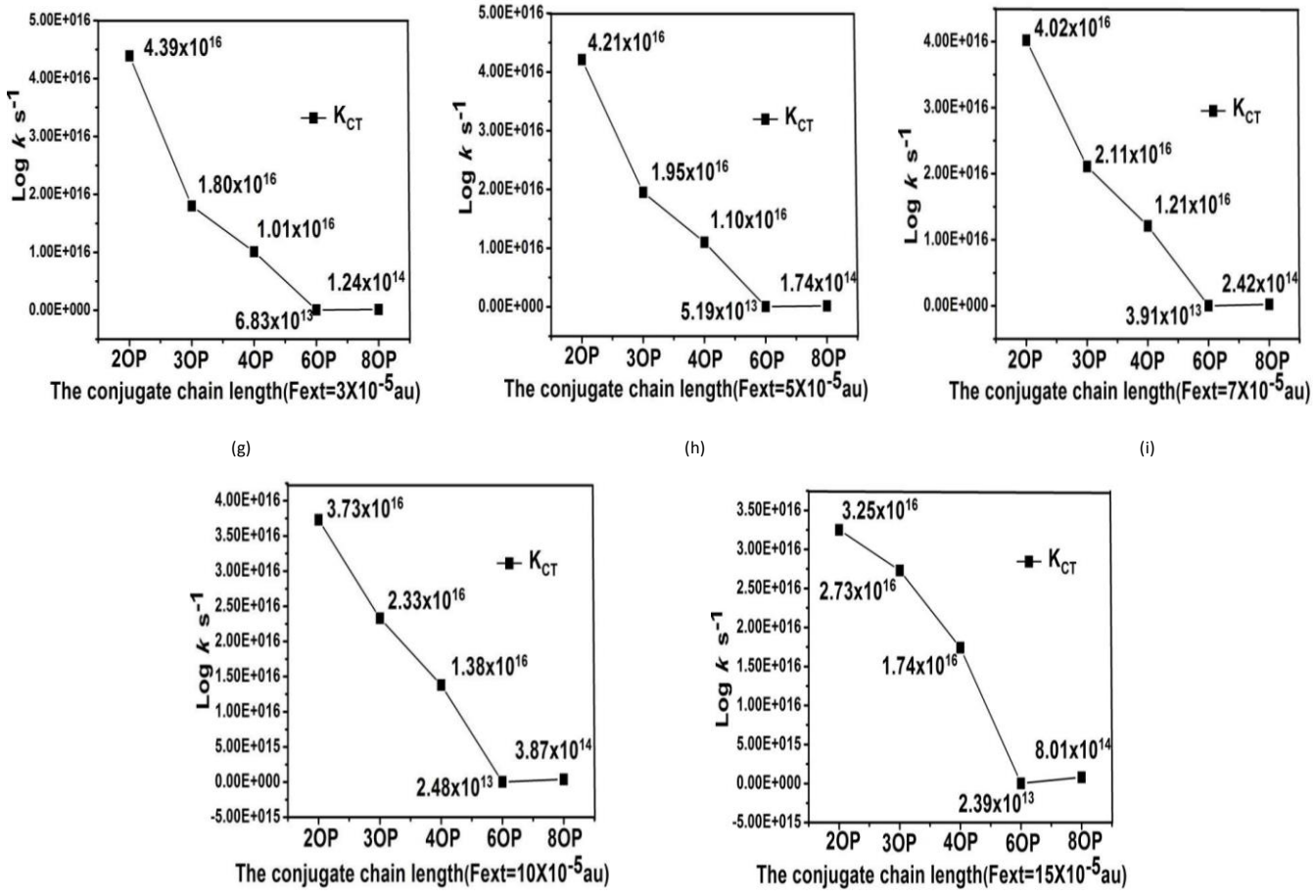

Figure S7: The k_{CT} in the system at different external electric fields.

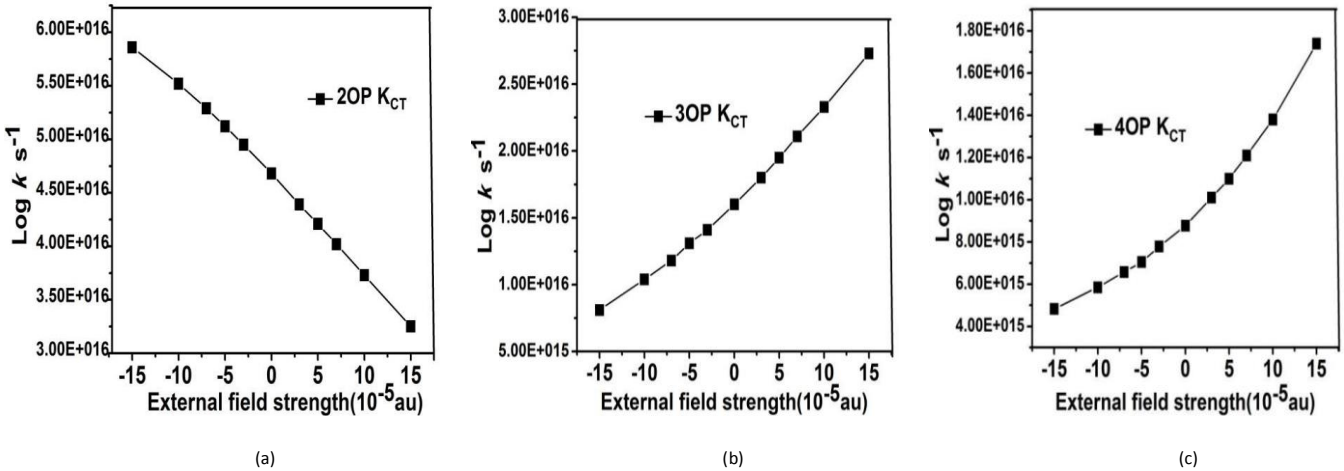

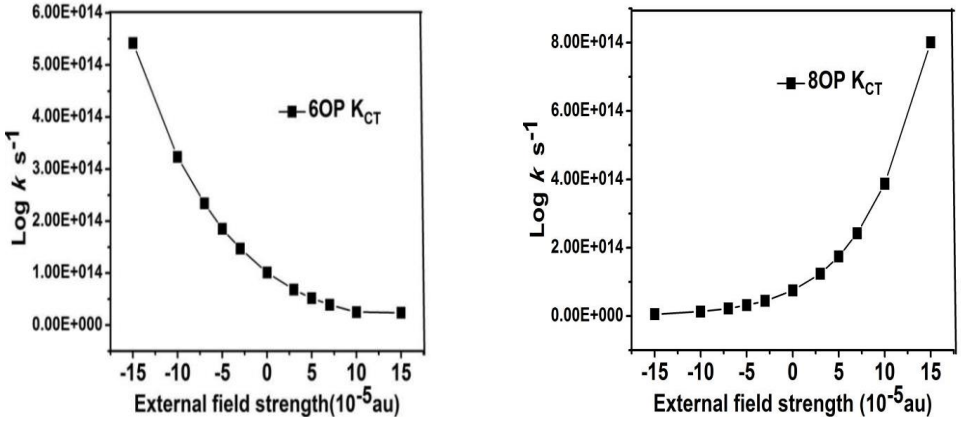

(d) (e)

Figure S8: The k_{CT} in the system at different conjugated chain length.